Cellular/Molecular

Deletion of *Kv4.2* Gene Eliminates Dendritic A-Type K^+ Current and Enhances Induction of Long-Term Potentiation in Hippocampal CA1 Pyramidal Neurons

Xixi Chen,[1]* Li-Lian Yuan,[2]* Cuiping Zhao,[2] Shari G. Birnbaum,[3] Andreas Frick,[4] Wonil E. Jung,[5] Thomas L. Schwarz,[5,6] J. David Sweatt,[7] and Daniel Johnston[1]

[1]Center for Learning and Memory, University of Texas at Austin, Austin, Texas 78712, [2]Department of Neuroscience, University of Minnesota, Minneapolis, Minnesota 55455, [3]Department of Psychiatry, University of Texas Southwestern Medical Center, Dallas, Texas 75390, [4]Department of Cell Physiology, Max Plank Institute for Medical Research, D-69120 Heidelberg, Germany, [5]Department of Molecular and Cellular Physiology, Stanford University, Stanford, California 94305, [6]Program in Neurobiology, Children's Hospital, Harvard Medical School, Boston, Massachusetts 02115, and [7]Department of Neurobiology, University of Alabama at Birmingham, Birmingham, Alabama 35294

Dendritic, backpropagating action potentials (bAPs) facilitate the induction of Hebbian long-term potentiation (LTP). Although bAPs in distal dendrites of hippocampal CA1 pyramidal neurons are attenuated when propagating from the soma, their amplitude can be increased greatly via downregulation of dendritic A-type K^+ currents. The channels that underlie these currents thus may represent a key regulatory component of the signaling pathways that lead to synaptic plasticity. We directly tested this hypothesis by using *Kv4.2* knock-out mice. Deletion of the *Kv4.2* gene and a loss of Kv4.2 protein resulted in a specific and near-complete elimination of A-type K^+ currents from the apical dendrites of CA1 pyramidal neurons. The absence of dendritic *Kv4.2*-encoded A-type K^+ currents led to an increase of bAP amplitude and an increase of concurrent Ca^{2+} influx. Furthermore, CA1 pyramidal neurons lacking dendritic A-type K^+ currents from *Kv4.2* knock-out mice exhibited a lower threshold than those of wild-type littermates for LTP induction with the use of a theta burst pairing protocol. LTP triggered with the use of a saturating protocol, on the other hand, remained indistinguishable between *Kv4.2* knock-out and wild-type neurons. Our results support the hypothesis that dendritic A-type K^+ channels, composed of Kv4.2 subunits, regulate action potential backpropagation and the induction of specific forms of synaptic plasticity.

Key words: **K^+ channels; long-term potentiation; hippocampus; dendrites; backpropagating action potential; knock-out mouse**

Introduction

Correlated presynaptic and postsynaptic activity results in long-term changes in synaptic strength. The phenomenon is known as Hebbian-type plasticity (Magee and Johnston, 1997; Markram et al., 1997; Bi and Poo, 1998; Debanne et al., 1998; Sjostrom et al., 2001; Golding et al., 2002; Watanabe et al., 2002). A common factor in the induction of Hebbian-type long-term potentiation (LTP) is the necessity of postsynaptic depolarization, which facilitates NMDA receptor activation and the activation of voltage-dependent Ca^{2+} channels, both of which lead to a Ca^{2+} rise in the postsynaptic neuron (Magee and Johnston, 1997; Golding et al., 2002; Frick et al., 2004; Lisman and Spruston, 2005). One of the physiological mechanisms of postsynaptic depolarization is the backpropagating action potential (bAP), which usually is generated in the axon and backpropagates into the dendrites (Stuart and Sakmann, 1994; Spruston et al., 1995). Pairing of bAPs and EPSPs can result in supralinear summation in the dendrites of membrane voltage (Magee and Johnston, 1997; Stuart and Hausser, 2001) and of Ca^{2+} influx (Yuste and Denk, 1995; Magee and Johnston, 1997; Koester and Sakmann, 1998; Mainen et al., 1999; Nevian and Sakmann, 2004), leading to the induction of LTP (Magee and Johnston, 1997; Markram et al., 1997; Watanabe et al., 2002; Frick et al., 2004; Fan et al., 2005). bAPs in the dendrites of hippocampal CA1 pyramidal neurons are an essential feature for the induction of LTP of the Schaffer collateral pathway under physiological conditions (Magee and Johnston, 1997). It is therefore conceivable that regulators of bAPs also regulate the induction of LTP.

In the CA1 pyramidal neurons of hippocampus the amplitude of these bAPs decreases as they travel farther away from the soma (Spruston et al., 1995; Magee and Johnston, 1997; Yuan et al., 2002; Bernard and Johnston, 2003; Frick et al., 2004), despite the uniform density of voltage-dependent Na^+ channels (Magee and Johnston, 1995). In contrast, the density of the A-type K^+ currents increases along the apical dendrites (Hoffman et al., 1997). The location and properties of the A-type K^+ currents make them suitable as key regulators of action potential backpropaga-

Received June 23, 2006; revised Oct. 3, 2006; accepted Oct. 10, 2006.

This work was supported by National Institutes of Health Grants NS37444, MH48432, MH44754 (D.J.), MH70857 (L.-L.Y.), and MH57014 (J.D.S.). We thank Dr. Andreas Jeromin, Yunqing Han, and Amber Lockridge for genotyping and maintaining the mouse colonies and Dr. James Trimmer for the gift of some antibodies.

*X.C. and L.-L.Y. contributed equally to this work.

Correspondence should be addressed to Daniel Johnston, Center for Learning and Memory, University of Texas at Austin, Austin, TX 78712. E-mail: djohnston@mail.clm.utexas.edu.

DOI:10.1523/JNEUROSCI.2667-06.2006

 0270-6474/06/2612143-09$15.00/0

tion (Hoffman and Johnston, 1998; Watanabe et al., 2002; Yuan et al., 2002; Chen and Johnston, 2004).

A-type K^+ currents in CA1 pyramidal neurons can be encoded by either the *Kv1.4* or *Kv4.2* gene (Coetzee et al., 1999). However, based on immunohistochemistry studies, the Kv1.4 proteins are found primarily in the axon, whereas the Kv4.2 proteins are found mostly in the dendrites (Sheng et al., 1992; Gu et al., 2003). Consistent with this localization and in the context of synaptic plasticity in CA1 pyramidal neurons, the threshold of LTP induction of field EPSPs is lowered by heteropodatoxin 3 (HpTX3), a relatively selective blocker of Kv4 channels (Ramakers and Storm, 2002).

In this report, we investigated a key test of the overall hypothesis linking dendritic A-type K^+ current, action potential backpropagation, and LTP induction by evaluating the physiology of CA1 pyramidal neurons in mice specifically lacking the *Kv4.2* gene. Previous studies show that transient K^+ currents in cardiac myocytes and spinal cord dorsal horn neurons are reduced in these *Kv4.2*$^{-/-}$ mice (Jung, 2002; Guo et al., 2005; Hu et al., 2006). This report focuses on the CA1 region of hippocampus.

Materials and Methods

Transgenic animals and genotyping

Kv4.2$^{-/-}$ mice were generated in 129/SvEv background (Guo et al., 2005). Littermate genotypes were confirmed by PCR results on the basis of *Kv4.2*-specific primers (forward, GTG GAT GCC TGT TGC TTC; reverse, CCC ACA AGG CAG TTC TTT TA) and *neo*-specific primers (forward, AGG ATC TCC TGT CAT CTC ACC TTG CTC CTG; reverse, AAG AAC TCG TCA AGA AGG CGA TAG AAG GCG).

Preparation of acute hippocampal slices from mouse brain

Hippocampal slices were prepared from 5- to 12-week-old mice by following standard procedures. Briefly, the animals were anesthetized by lethal dose of a mix of ketamine and xylazine and perfused through the heart with ice-cold cutting solution containing the following (in mM): 240 sucrose, 2.5 KCl, 1.25 NaH_2PO_4, 25 $NaHCO_3$, 0.5 $CaCl_2$, and 7 $MgCl_2$, saturated with 95% O_2/5% CO_2 before freezing. Both hemispheres then were removed quickly and sliced at 350 μm in thickness with a vibratome. After incubation in a holding chamber for at least 30 min at room temperature, the slices were transferred into the recording chamber. Both the holding and the recording chambers contained the following (in mM): 125 NaCl, 2.5 KCl, 1.25 NaH_2PO_4, 25 $NaHCO_3$, 2.0 $CaCl_2$, 1.0 $MgCl_2$, and 25 dextrose.

Organotypic culture of mouse hippocampus

Mouse organotypic slices were prepared and cultured according to the interface technique (Stoppini et al., 1991). Slices were prepared from postnatal day 1–7 mice at 325 μm thickness with a McIlwain tissue chopper (Mickle Laboratory Engineering, Guildford, Surrey, UK) and cultured on Millicell inserts (Millipore, Bedford, MA) in a MEM-based medium (Invitrogen, Carlsbad, CA) containing 20% horse serum (Invitrogen). Medium was changed every 2 d, and the slices could be kept alive for at least 4 weeks in culture.

Electrophysiological recordings

A Zeiss Axioskop (Oberkochen, Germany) fit with a 40 or 60× water immersion objective and differential interference contrast (DIC) was used to view the slices. Light in the near-infrared (IR) range (740 nm) in conjunction with a contrast-enhancing camera was used to visualize individual dendrites. An Axopatch-200 or Axopatch-1D amplifier was used for voltage-clamp recordings. Current-clamp recordings were performed by using either an Axoclamp-2A or a BVC700A amplifier. Whole-cell recording pipettes (7–12 MΩ) contained the following (in mM): 120 $KMeSO_4$ or 120 K-gluconate, 20 KCl, 10 HEPES, 0.2 EGTA, 8 NaCl, 4 Mg-ATP, 0.3 Tris-GTP, and 14 phosphocreatine (pH 7.25-adjusted with KOH). For cell-attached patch recordings the pipettes (10–14 MΩ) were wrapped with Parafilm to reduce pipette capacitance; the tips were inspected visually for uniform diameter (~1 μm) and were fire polished. Pipette solution for cell-attached recording of voltage-dependent K^+ channels contained the following (in mM): 125 NaCl, 10 HEPES, 2 $CaCl_2$, 1 $MgCl_2$, and 2.5 KCl plus 1 μM TTX (pH 7.4-adjusted with KOH). To isolate whole-cell voltage-dependent K^+ currents in pyramidal neurons, we added 1 μM TTX and 2 mM $MnCl_2$ to the bath solution with 0 Ca^{2+} and 0 NaH_2PO_4 to block Na^+ currents, Ca^{2+} currents, and Ca^{2+}-activated K^+ currents. Pulse generation and data acquisition were controlled with custom software written in the IgorPro environment. Linear leak and capacitive currents were subtracted digitally by using null traces or scaled traces of smaller voltage steps.

To induce LTP, we paired subthreshold synaptic stimulation and postsynaptic action potentials (APs). Schaffer collateral fibers were stimulated electrically with a bipolar microelectrode placed in stratum radiatum at a lateral distance of 50–100 μm from the apical dendrite. Axonally initiated APs were elicited with somatic depolarizing current injection or antidromic stimulation via a stimulating electrode in the alveus. Test stimuli were delivered every 20–30 s; a hyperpolarizing current pulse was injected into the cell after the test stimulus to monitor input resistance and series resistance. Slope measurements of EPSP were made from a line fit to the rising phase of the EPSP. The magnitude of potentiation was quantified by averaging the slope of EPSP rising phase for a 10 min period between 20 and 30 min after induction and dividing this number by the average slope of EPSP rising phase during the 10 min baseline before induction. During LTP induction the number of APs actually fired by the cell did not always match the number of stimuli (current injections or antidromic stimuli). The actual number of APs fired by the cell was counted, and an average per burst was calculated for every experiment.

Whole-cell voltage-clamp recordings in organotypic slice culture were performed at room temperature (22–24°C). In acute slices the cell-attached voltage-clamp recordings were performed at room temperature (22–24°C); whole-cell current-clamp recordings were performed at near-physiological temperature (32–34°C). Dendritic recordings were made from the trunk of the apical dendrites. We performed whole-cell voltage-clamp experiments in organotypic slice cultures because cells in this preparation are electrotonically more compact than cells in acute slices. This allows us to have a better estimation of the amplitude of whole-cell current with voltage clamp (Johnston and Brown, 1983; Jeromin et al., 2003). We performed all of the voltage-clamp experiments at room temperature instead of near-physiological temperature because of better stability of the recordings (in both the whole-cell and the cell-attached configuration). With the whole-cell configuration this also allows for better voltage clamp because of slower kinetics (Johnston and Brown, 1983).

Ca^{2+} imaging

We performed Ca^{2+} fluorescence imaging in a similar way to that described previously (Frick et al., 2003). A Quantix 57 CCD camera (Roper Scientific, Duluth, GA) with a 535 × 512 pixel array and single wavelength (380 nm) excitation was used, with changes in $[Ca^{2+}]_i$ quantified by calculating $\Delta F/F$, where F is the fluorescence intensity before stimulation (after subtracting autofluorescence) and ΔF is the change in fluorescence during neuronal activity (corrected for bleaching). The autofluorescence of the tissue was measured in a region of equal size but adjacent to the dye-filled neuron, either in the dendritic field or in the cell body layer, and bleaching was determined by measuring the change in fluorescence at rest (without stimulation). The $\Delta F/F$ measurements usually were repeated four to six times and averaged. Sequential frame rate was 50–100 Hz, and pixels were binned in a 5 × 5 array. To reach the equilibrium state of dye diffusion, we typically waited at least 20 min after break-in to allow the indicator dye (bis-fura-2) to diffuse into the most distal part of the cell before we recorded optical signals. The distance of any given location along an apical dendrite was measured from the base of apical dendrites. Ca^{2+} imaging experiments were performed at near-physiological temperature (32–34°C).

Wild-type controls

For organotypic slice culture the non-littermate wild-type 129/SvEv mice were used as controls. Gender of the animals could not be differentiated at the time of culture.

For experiments in acute slices both non-littermate and littermate wild-type 129/SvEv mice were used as controls in recordings of dendritic K^+ currents, bAPs, and Ca^{2+} signals. Age-matched littermate controls were used for LTP experiments. Male mice were used for experiments in acute slices.

Biochemical analysis

Sample preparation. Adult mice (129S6/SvEvTaq or *Kv4.2* knock-out mice) were decapitated, and their brains were placed rapidly into ice-cold cutting saline [containing the following (in mM): 110 sucrose, 60 NaCl, 3 KCl, 1.25 NaH_2PO_4, 28 $NaHCO_3$, 7 $MgCl_2$, 0.5 $CaCl_2$, 5 glucose, and 0.6 ascorbate, saturated with 95% O_2/5% CO_2]. Then the brain regions of interest were removed, immediately frozen on dry ice, and stored at –80°C until assayed.

The hippocampi were homogenized and briefly sonicated in ~600 μl of ice-cold homogenization buffer [containing the following (in mM): 20 Tris, pH 7.5, 1 EGTA, 1 EDTA, 1 $Na_4P_2O_7$, 4 para-nitrophenylphosphate, and 1 sodium orthovanadate plus 100 μM phenylmethylsulfonyl fluoride and 10 μl/ml protease inhibitor mixture (Sigma-Aldrich, St. Louis, MO)]. Membrane fractions were prepared. The samples were centrifuged at 1000 × *g* for 5 min to remove cellular debris; then the supernatant was centrifuged at 100,000 × *g* for 30 min. The pellet was resuspended in 5% SDS in homogenization buffer. The protein content of each sample was assessed (DC protein assay; Bio-Rad, Hercules, CA), and SDS/homogenization buffer was added to normalize the protein level between samples. Sample buffer (0.3 M Tris, pH 6.8, 40% glycerol, 8% SDS, and 150 mM dithiothreitol) was added, and the samples were stored at –20°C. Samples were loaded onto 10% SDS-polyacrylamide gels and resolved by standard electrophoresis. Gels were transferred electrophoretically to Immobilon polyvinylidene difluoride membranes.

Western blotting. Immobilon filters were blocked for 1 h at room temperature in 5% dry milk and 3% bovine serum albumin dissolved in Tween–Tris-buffered saline (TTBS; 50 mM Tris, pH 7.5, 150 mM NaCl, 1 μM microcystin, 0.1% Tween 20) or 0.2% I-Block in TTBS. The blots were incubated for either 1 h at room temperature or overnight at 4°C with the primary antibody and then were washed four times (10 min each) with TTBS. Blots were incubated with an HRP-conjugated anti-rabbit (1:20,000; Cell Signaling Technology, Beverly, MA) or anti-mouse (1:20,000; Cell Signaling Technology) secondary antibody and then washed four times with TTBS. The blots were developed with Enhanced Chemiluminescence (Amersham Biosciences, Arlington Heights, IL) and visualized on film [Kodak BioMax MR (Rochester, NY) or ISC BioExpress Blue Lite (Kaysville, UT)]. Primary antibodies that were used included Kv4.3, Kv1.4, Kv3.4, and the H channel proteins HCN1 and HCN2 (1:500, 1:500, 1:200, 1:500, 1:500, respectively; Chemicon, Temecula, CA); glutamate receptors GluR1 and GluR2/3 (1:1000; Upstate Biotechnology, Lake Placid, NY); K^+ channel-interacting proteins KChIP1, KChIP2, and KChIP3 (1:3500, 1:2500, 1:100, respectively; gifts from Dr. J. Trimmer, University of California, Davis, CA); postsynaptic density-95 (PSD-95; 1:1000; Zymed, San Francisco, CA); synapse-associated protein 97 (SAP97; 1:3000; Affinity BioReagents, Neshanic Station, NJ); neuronal calcium sensor protein 1 (NCS1; 1:1000; Santa Cruz Biotechnology, Santa Cruz, CA); dipeptidyl peptidase X (DPPX; 1:500; a gift from Dr. W. Cookson, Oxford University, Oxford, UK); and pentraxin 3 (PTX3; 1:1000; Axxora, San Diego, CA). Blots were stripped of the original antibody by being washed twice with 0.2 M NaOH (20 min each) and then four times in TTBS. Western blotting was repeated on the same blots with an anti-actin antibody (1:1000; Sigma–Aldrich) to ensure equal loading between lanes. Densitometric analysis of immunoreactivity was conducted with a desktop scanner and NIH ImageJ software (Bethesda, MD).

Statistical analysis

Significance ($p < 0.05$) was determined with two-sample Student's *t* tests. Error bars represent the SEM.

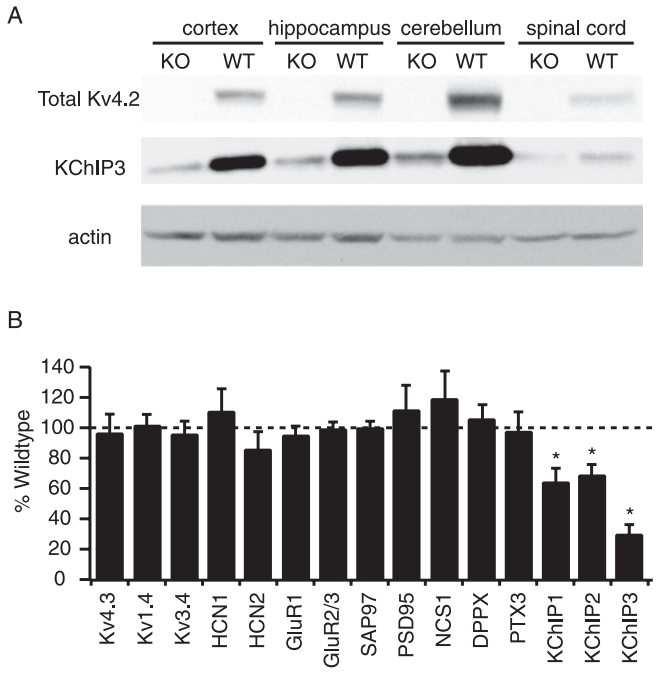

Figure 1. Absence of Kv4.2 protein and reduced expression level of KChIPs in *Kv4.2* $^{-/-}$ mice. ***A***, Western blotting confirmed the absence of Kv4.2 protein in various CNS regions of *Kv4.2* $^{-/-}$ mice, including cortex, hippocampus, cerebellum, and spinal cord [$n = 9$ of wild-type (WT); $n = 9$ of *Kv4.2* $^{-/-}$ (KO)]. ***B***, The absence of Kv4.2 protein was accompanied by a significant decrease of KChIPs in *Kv4.2* $^{-/-}$ mice. Kv4.3: $n = 9$ of wild-type, $n = 8$ of *Kv4.2* $^{-/-}$; Kv1.4, HCN1, and HCN2: $n = 9$ of wild-type, $n = 9$ of *Kv4.2* $^{-/-}$; Kv3.4: $n = 7$ of wild-type, $n = 7$ of *Kv4.2* $^{-/-}$; GluR1 and GluR2/3: $n = 7$ of wild-type, $n = 7$ of *Kv4.2* $^{-/-}$; SAP97, PSD-95, and NCS1: $n = 4$ of wild-type, $n = 4$ of *Kv4.2* $^{-/-}$; DPPX and PTX3: $n = 8$ of wild-type, $n = 8$ of *Kv4.2* $^{-/-}$; KChIP1, KChIP2, and KChIP3: $n = 7$ of wild-type, $n = 7$ of Kv4.2 $^{-/-}$. Error bars represent the SEM; $^*p < 0.05$.

Results

Deleting the *Kv4.2* gene led to abolishment of Kv4.2 protein in the brain and spinal cord

The *Kv4.2* knock-out (*Kv4.2* $^{-/-}$) mouse was generated by targeted disruption of exon I of the *Kv4.2* gene (Guo et al., 2005). We performed Western blot analysis on total protein extracted from the cortex, hippocampus, cerebellum, and spinal cord of *Kv4.2* $^{-/-}$. Tissue from age-matched wild-type mice (*Kv4.2* $^{+/+}$) of the same genetic background was used as control. As expected, the Kv4.2 protein was detected at high levels in various brain regions of control mice but was undetectable in *Kv4.2* $^{-/-}$ mice (Fig. 1*A*).

Expression levels of 15 other proteins in the hippocampus also were analyzed with Western blotting, including other K^+ channel proteins potentially underlying neuronal A-type K^+ currents: Kv4.3, Kv1.4, and Kv3.4; the H channel proteins HCN1 and HCN2; the AMPA-type glutamate receptor proteins GluR1 and GluR2/3; two membrane-anchoring proteins enriched in the postsynaptic area, SAP97 and PSD-95; and proteins that functionally or physically associate with Kv4.2 such as NCS1, DPPX, a secretory-type protein containing a pentraxin domain (PTX3), and KChIP1, KChIP2, and KChIP3 (Rhodes et al., 2004; Menegola and Trimmer, 2006). The protein levels of KChIP1, KChIP2, and KChIP3 were reduced significantly, by 30–70%, in the hippocampus of *Kv4.2* $^{-/-}$ mice as compared with wild type. Levels of the other proteins were not altered significantly in *Kv4.2* $^{-/-}$ (Fig. 1*B*). These data confirm a complete loss of CNS Kv4.2 protein in *Kv4.2* knock-out animals. Moreover, these findings suggest an inter-

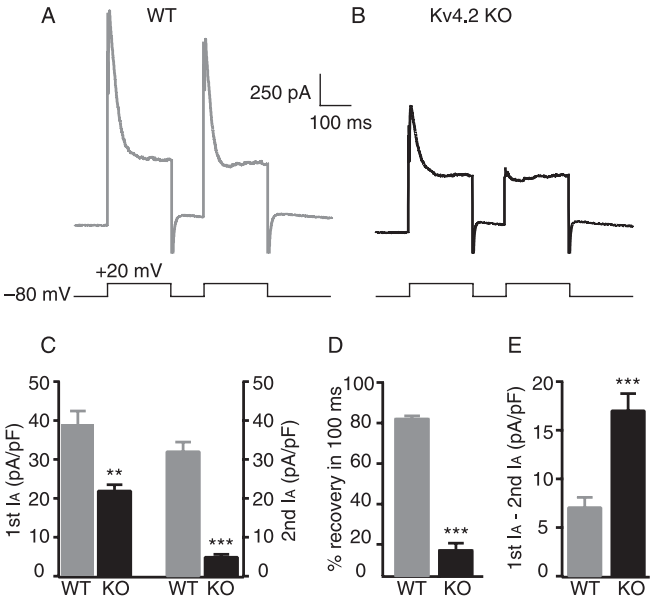

Figure 2. Reduction of Kv4-mediated and upregulation of Kv1-mediated whole-cell A-type K^+ current in *Kv4.2*$^{-/-}$. Whole-cell voltage-clamp recordings were performed from the soma of CA1 pyramidal neurons in organotypic slice cultures. ***A***, CA1 pyramidal neurons from wild-type (WT) mice exhibited a prominent portion of the transient A-type K^+ current, which recovered from inactivation to 82.2% within 100 ms, indicating that >80% of native A-type current was from Kv4. ***B***, Under the same condition there was a significant reduction of the first transient amplitude and an even further reduction of the second transient amplitude in *Kv4.2*$^{-/-}$ (***C***). ***D***, As a result, there was a <20% recovery of A-type current within 100 ms in *Kv4.2*$^{-/-}$. The difference between the first and the second transient amplitude reflected the amount of transient current that did not recover from inactivation within 100 ms and, thus, was not mediated by Kv4 subunits. ***E***, The non-Kv4-mediated current was upregulated significantly in *Kv4.2*$^{-/-}$. The sustained component of K^+ currents in CA1 pyramidal neurons remained the same between WT and *Kv4.2*$^{-/-}$ mice. Error bars represent the SEM; $^{**}p < 0.01$; $^{***}p < 0.005$.

esting coordinate regulation of Kv4.2 and KChIP1, KChIP2, and KChIP3 (Menegola and Trimmer, 2006).

Differential changes in the Kv1- and Kv4-mediated components of whole-cell A-type K^+ currents in *Kv4.2*$^{-/-}$

Both the *Kv1* and *Kv4* families of K^+ channel genes are expressed in CA1 pyramidal neurons. Kv1- and Kv4-mediated A-type K^+ currents differ in the kinetics of recovery from inactivation (Coetzee et al., 1999). The time course of recovery from inactivation of Kv4 channels and dendritic A-type current ($\tau < 100$ ms) (Johnston et al., 2000; Jerng et al., 2004) is faster than that of Kv1 channels ($\tau > 1$ s) (Castellino et al., 1995) by an order of magnitude. Hence the relative contributions of Kv1 channels and Kv4 channels to whole-cell A-type K^+ currents can be studied with a voltage protocol that takes advantage of their difference in recovery from inactivation.

Figure 2 illustrates such a protocol. Whole-cell voltage-clamp recordings were performed from the soma of CA1 pyramidal neurons in organotypic slice cultures. The membrane potential was held at −80 mV, and two identical voltage steps to +20 mV with a duration of 200 ms and interval of 100 ms were applied to activate voltage-dependent K^+ channels. In wild-type neurons the first depolarizing step activated whole-cell K^+ currents with an A-type component that fully inactivated at the end of the 200 ms step. During the 100 ms hyperpolarization between the two depolarizing steps a large portion of the A-type current recovered from inactivation. The amplitude of the first transient (peak current subtracted by the non-inactivating component) represents the total amount of whole-cell A-type current. The amplitude of the second transient represents the amount of whole-cell A-type current that is mediated by Kv4 channels. The difference between the first transient and the second transient represents the amount of Kv1-mediated current that would not be expected to recover from inactivation during the 100 ms hyperpolarization (Varga et al., 2004).

In comparison to the wild-type neurons (39.14 ± 3.30 pA/pF; $n = 6$), CA1 pyramidal neurons of *Kv4.2*$^{-/-}$ had a significantly reduced amount of total A-type K^+ currents (21.97 ± 1.54 pA/pF; $n = 10$). The Kv4-mediated A-type current (as revealed by the second voltage step), in particular, was mostly absent in *Kv4.2*$^{-/-}$ neurons (4.94 ± 0.68 pA/pF in knock-out as compared with 32.06 ± 2.41 pA/pF in wild type). However, the A-type current component that did not recover within 100 ms, quantified as the difference between the first and the second transient, was 7.08 ± 1.02 pA/pF ($n = 6$) in wild-type and 17.03 ± 1.74 pA/pF ($n = 10$) in CA1 pyramidal neurons of *Kv4.2*$^{-/-}$. The whole-cell capacitance was not different between wild-type (26.5 ± 2.3 pF; $n = 6$) and *Kv4.2*$^{-/-}$ (29.2 ± 2.1 pF; $n = 10$) neurons. These results suggest that, although total Kv1.4 protein amount appears to be unchanged in whole hippocampus in *Kv4.2*$^{-/-}$ (Fig. 1), some non-Kv4 subunits, most likely Kv1 family members, are upregulated in *Kv4.2*$^{-/-}$, at least in CA1 neurons (Fig. 2*C–E*).

Dendritic A-type K^+ current was eliminated specifically and completely in *Kv4.2*$^{-/-}$

We next asked whether the dendritic A-type K^+ current was affected by the loss of Kv4.2. Cell-attached recordings of macroscopic voltage-dependent K^+ currents were made from the dendrites of *Kv4.2*$^{-/-}$ and wild-type mice in acute slices. The results are illustrated in Figure 3. In CA1 dendrites the macroscopic K^+ currents usually are composed of a transient A-type component and a sustained component (Hoffman et al., 1997), and the amplitude of both components varies considerably (Chen and Johnston, 2004). In the *Kv4.2*$^{-/-}$ dendrites, however, macroscopic K^+ currents did not have a transient component that could be measured reliably (Fig. 3*A*). In wild-type dendrites 200–300 μm from soma the peak A-type current had an amplitude of 15.0 ± 4.1 pA (distance from soma, 225 ± 9 μm; $n = 15$), whereas in *Kv4.2*$^{-/-}$ dendrites at comparable distances from the soma the peak transient had an amplitude of 1.4 ± 0.5 pA (distance from soma, 241 ± 8 μm; $n = 11$; $p = 0.005$) (Fig. 3*B*). The sustained component of macroscopic K^+ currents did not seem to be different between wild-type (6.7 ± 1.4 pA; $n = 15$) and *Kv4.2*$^{-/-}$ dendrites (5.2 ± 1.0 pA; $n = 11$; $p = 0.381$) (Fig. 3*C*). Thus A-type K^+ current was eliminated specifically in dendrites of CA1 pyramidal neurons of *Kv4.2*$^{-/-}$. Although compensation from the upregulation of other Kv channel-mediated A-type current was detected at the whole-cell level (Fig. 2), such compensation did not appear to occur in the apical dendrite.

bAPs in dendrites were of larger amplitude in *Kv4.2*$^{-/-}$

To test whether the lack of dendritic A-type current affected dendritic APs, we recorded bAPs in the dendrites of *Kv4.2*$^{-/-}$ CA1 neurons and wild-type controls. Figure 4*A* shows examples of recordings in the soma and in dendrites 250 μm from the soma. Recordings were performed at near-physiological temperature (32–34°C). When recorded in the range of 220–300 μm along the dendrite in wild-type neurons (distance from soma, 238 ± 4 μm; $n = 19$), the amplitude of the bAPs was 29.8 ± 1.2 mV ($n = 19$). At comparable locations (distance from soma, 246 ± 6 μm; $n = 15$) and temperature the bAP amplitude (57.9 ± 2.6 mV; $n = 15$)

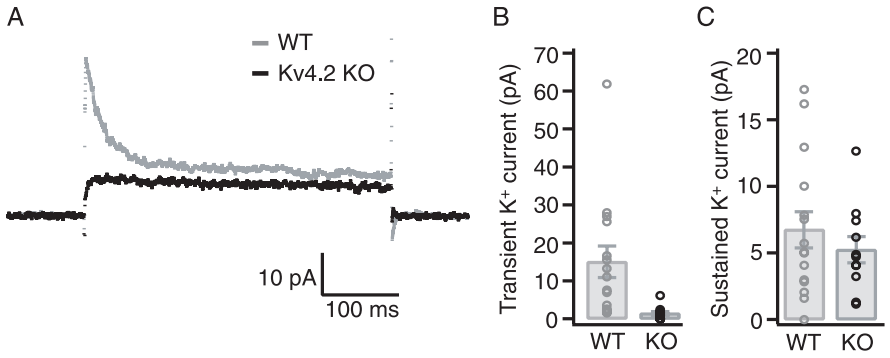

Figure 3. Cell-attached recordings revealed the absence of dendritic A-type K$^+$ current in CA1 pyramidal neurons of *Kv4.2*$^{-/-}$. Cell-attached voltage-clamp recordings were performed from the trunk of the apical dendrites of CA1 pyramidal neurons in acute slices. ***A***, In wild-type (WT) mice there was prominent A-type current in the apical dendrites (200–300 μm from soma) of CA1 pyramidal neurons, which we recorded as the transient component of total K$^+$ current with a voltage step from −100 to +50 mV. This component was missing in the dendrites of *Kv4.2*$^{-/-}$ mice. ***B***, In WT dendrites, the amplitude of A-type current was 15 ± 4.1 pA ($n = 15$; 11 from non-littermate controls and 4 from littermate controls). In *Kv4.2*$^{-/-}$ the amplitude of A-type current was 1.4 ± 0.5 pA ($n = 11$; 7 from non-littermate *Kv4.2*$^{-/-}$ and 4 from littermate *Kv4.2*$^{-/-}$). ***C***, The amplitude of the sustained K$^+$ current was not altered in dendrites of *Kv4.2*$^{-/-}$. In WT dendrites the amplitude of the sustained current was 6.7 ± 1.4 pA (same cells as in ***B***). In Kv4.2$^{-/-}$ the amplitude of the sustained current was 5.2 ± 1.0 pA (same cells as in ***B***).

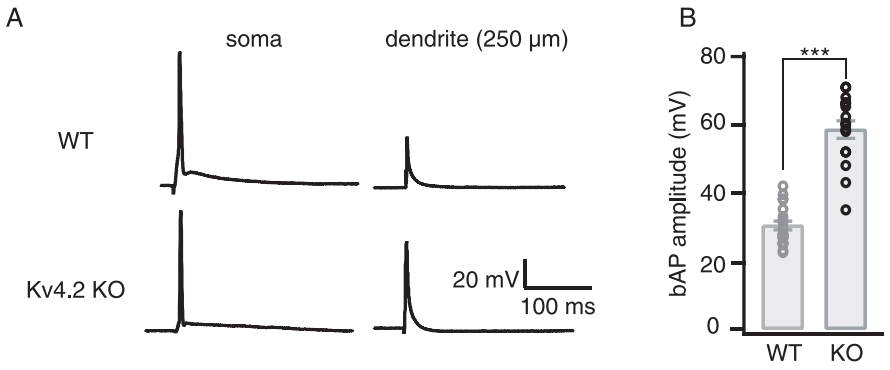

Figure 4. Elimination of dendritic A-type K$^+$ current resulted in larger dendritic bAPs in *Kv4.2*$^{-/-}$ mice. Whole-cell current-clamp recordings were performed from CA1 pyramidal neurons in acute slices. ***A***, Comparison of bAP amplitude between wild-type (WT) and *Kv4.2*$^{-/-}$. APs recorded from soma showed no significant difference between *Kv4.2*$^{-/-}$ and WT controls. At 250 μm from soma the amplitude of bAP was larger in *Kv4.2*$^{-/-}$ as compared with WT. ***B***, At comparable distances from the soma (220–300 μm) the amplitude of bAP was 29.8 ± 1.2 mV in WT dendrites ($n = 19$; 15 from non-littermate controls and 4 from littermate controls) and 57.9 ± 2.6 mV in *Kv4.2*$^{-/-}$ ($n = 15$; 11 from non-littermate *Kv4.2*$^{-/-}$ and 4 from littermate *Kv4.2*$^{-/-}$). ***$p < 0.005$.

was significantly larger in *Kv4.2*$^{-/-}$ than in wild-type dendrites ($p \ll 0.001$) (Fig. 4*A*,*B*).

Additional analysis of bAPs revealed no difference in initial *dV*/*dt* between *Kv4.2*$^{-/-}$ (21.1 ± 2.8 mV/ms; $n = 14$) and wild-type neurons (20.6 ± 1.8 mV/ms; $n = 16$; $p = 0.86$), suggesting similar Na$^+$ channel activation (Colbert and Johnston, 1996). Maximum *dV*/*dt* was slightly larger in *Kv4.2*$^{-/-}$ [31.2 ± 2.6 mV/ms ($n = 14$) as compared with 26.1 ± 1.9 mV/ms in wild-type ($n = 16$)], but the difference was not statistically significant ($p = 0.12$). Half-width of bAPs was slightly shorter in *Kv4.2*$^{-/-}$ [4.9 ± 0.4 ms ($n = 14$) as compared with 6.0 ± 0.5 ms in wild-type ($n = 16$); $p = 0.11$], possibly as a consequence of the larger amplitude of bAPs that reached the activation threshold for other types of dendritic K$^+$ channels to participate in repolarization (Bernard and Johnston, 2003; Chen and Johnston, 2006).

Concurrent Ca^{2+} influx during bAPs was larger in *Kv4.2*$^{-/-}$

bAPs lead to Ca^{2+} influx in the dendrites via voltage-dependent Ca^{2+} channels (Yuste and Denk, 1995; Magee and Johnston, 1997). With larger bAPs propagating in the apical dendrites of CA1 pyramidal neuron of *Kv4.2*$^{-/-}$ mice, we tested whether this increase in voltage change in dendrites is translated into a similar increase of Ca^{2+} influx. CA1 pyramidal neurons were filled with bis-fura-2 (100 μM) during somatic whole-cell recordings. The amplitude of Ca^{2+} signals at multiple dendritic locations in the same neuron was monitored and quantified as $\Delta F/F$ while single APs were initiated with somatic current injection. Because the surface–volume ratio varies along the dendrites, the $\Delta F/F$ value as a function of dendritic location usually peaks at the proximal part of the apical dendrites (Regehr and Tank, 1992; Jaffe et al., 1994; Schiller et al., 1995). As previously described (Frick et al., 2003) in rat hippocampus, bAPs resulted in concurrent Ca^{2+} influx. The amount of Ca^{2+} rise at more distal dendritic locations (beyond 125 μm) decreased with distance from soma, in parallel with the decrement of bAP amplitude (wild type; $n = 8$) (Fig. 5). We chose 125 μm as the location to which we normalized the $\Delta F/F$ of various locations. Because bAPs were larger in *Kv4.2*$^{-/-}$ than in wild-type dendrites, Ca^{2+} signals should have less decrement along the dendrites of *Kv4.2*$^{-/-}$ neurons. This is indeed what we observed with Ca^{2+} imaging (Fig. 5). In *Kv4.2*$^{-/-}$ the bigger bAP amplitudes appeared to result in more Ca^{2+} influx (knock-out; $n = 7$) (Fig. 5).

Induction threshold of Hebbian-type LTP was lowered in *Kv4.2*$^{-/-}$

bAPs and concurrent Ca^{2+} influx in the dendrites are required for the induction of LTP with the theta burst pairing (TBP) protocol at the Schaffer collateral synapses of CA1 neurons (Magee and Johnston, 1997). The TBP protocol involves pairing of theta burst stimulation with postsynaptic current injection or antidromic stimulation to induce APs (Fig. 6*A*). The theta burst stimulation consists of five stimuli of the Schaffer collaterals at 100 Hz per burst and 10 repeats of the burst at the theta frequency (5 Hz) (Fig. 6*B*). A standard protocol to induce LTP reliably has each of the five EPSPs in every burst paired with a postsynaptic AP. In each pair of an EPSP plus AP, the stimulus for the EPSP usually precedes the stimulus for the AP by 7–8 ms (Frick et al., 2004; Fan et al., 2005). We used this protocol to try to induce LTP in CA1 neurons from *Kv4.2*$^{-/-}$ and their wild-type littermates. As is shown in Figure 6*C*, pairing the five EPSPs in every burst with three to five bAPs induced a similar magnitude of LTP in *Kv4.2*$^{-/-}$ (2.63 ± 0.35; $n = 7$) and wild-type littermate controls (2.53 ± 0.28; $n = 9$). This is consistent with previous studies that found no significant difference between *Kv4.2*$^{-/-}$ and control animals with respect to the amount of maximum LTP (Jung, 2002). Field EPSPs were recorded at room temperature in those studies, and a variety of LTP induction protocols were used (Jung, 2002).

It is known that, with TBP, LTP occurs only when sufficient

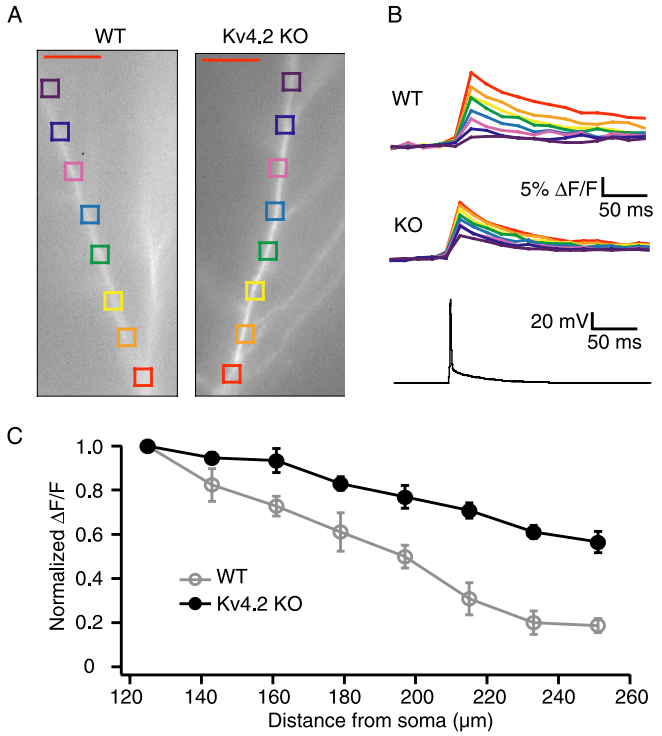

Figure 5. bAP-evoked Ca^{2+} signal in dendrites declined less with distance in *Kv4.2*$^{-/-}$. Whole-cell current-clamp recordings were performed from CA1 pyramidal neurons in acute slices. ***A***, Apical dendrites of CA1 pyramidal neurons were filled with 100 μM bis-fura-2. ***B***, In response to a brief current injection (2 nA for 2.5 ms) the neuron fired a single AP. Relative change of intracellular Ca^{2+} was quantified as $\Delta F/F$ at various locations on dendrites after bleach correction and autofluorescence subtraction. In wild-type (WT) $\Delta F/F$ declined at ~150 μm and almost reached 0 in distal dendrites (~250 μm). In contrast, the value in *Kv4.2*$^{-/-}$ stayed relatively high. ***C***, Normalized $\Delta F/F$ to that of dendritic location 125 μm was plotted as a function of distance from soma. Ca^{2+} influx caused by a single bAP in *Kv4.2*$^{-/-}$ ($n = 7$; 6 from non-littermate *Kv4.2*$^{-/-}$ and 1 from littermate *Kv4.2*$^{-/-}$) was much larger than that of WT ($n = 8$; 3 from non-littermate controls and 5 from littermate controls), and this difference was more obvious in distal dendrites. Error bars represent SEM.

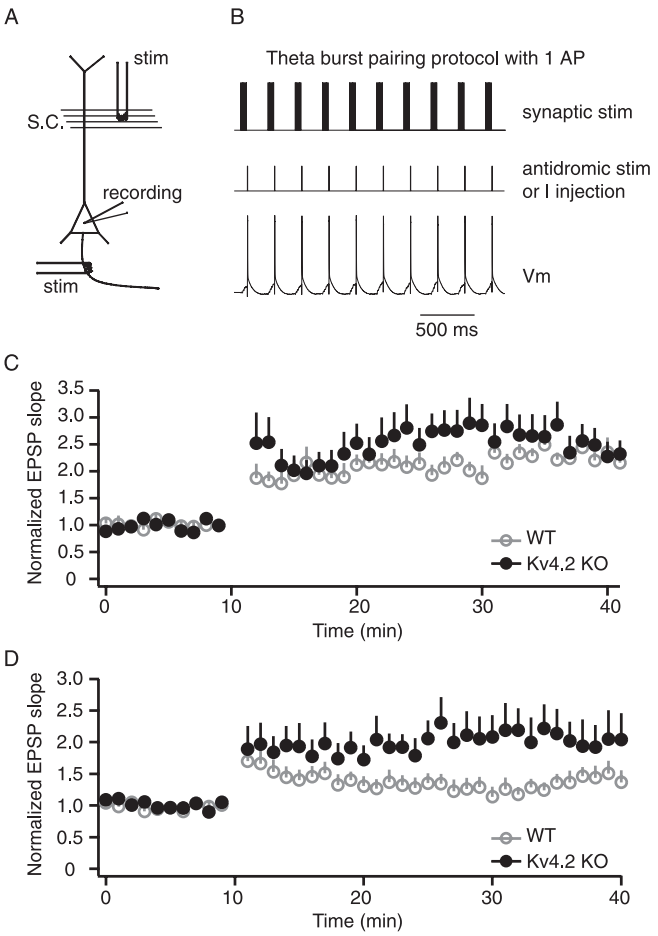

Figure 6. LTP induction was different in *Kv4.2*$^{-/-}$ and control littermates. Whole-cell current-clamp recordings were performed from CA1 pyramidal neurons in acute slices. ***A***, Experimental configuration. EPSPs were evoked by extracellular stimulation of Schaffer collateral pathways (S.C.). Postsynaptic APs were elicited either by brief, intracellular current injection or antidromic stimulation of pyramidal neuron axons. ***B***, TBP protocol in which one AP was paired with the fifth EPSP during a burst of five EPSPs. The five EPSPs within the burst were at 100 Hz. A train of stimuli consisted of 10 repeats of such bursts at 5 Hz. Five such trains of stimulation were applied repeatedly at a 12 s interval. The number of bAPs that paired with the EPSPs was varied in the experiments. ***C***, In response to a strong pairing protocol in which three to five APs were paired with five EPSPs in every burst, persistent LTP was induced in wild-type (WT; $n = 9$) and *Kv4.2*$^{-/-}$ ($n = 7$) mice. ***D***, In response to a relatively weak pairing protocol in which fewer than two APs were paired with EPSPs, LTP was of significantly larger magnitude in *Kv4.2*$^{-/-}$ ($n = 9$) than in control littermates ($n = 19$).

numbers of EPSPs and bAPs are paired in time (Watanabe et al., 2002). We reasoned that, because bAPs were larger in *Kv4.2*$^{-/-}$, these bAPs should be more effective than those of wild-type neurons in unblocking NMDA receptors and inducing LTP. As a consequence, fewer postsynaptic APs would be needed for LTP induction. We therefore adjusted the strength of induction in the TBP protocol by varying the number of APs that were paired with EPSPs.

When fewer than two APs on average were paired with EPSPs in a burst, LTP induction was significantly more robust in *Kv4.2*$^{-/-}$ (2.31 ± 0.38; $n = 9$) than in their wild-type littermates (1.27 ± 0.13; $n = 19$) (Figs. 6*D*, 7*A*). We consider >50% increase in the initial EPSP slope after 20 min of TBP as successful LTP. By this criterion, the likelihood of LTP induction with this smaller number of pairings was >60% in *Kv4.2*$^{-/-}$ and ~20% in wild-type (Fig. 7*A*). We further grouped the data according to the average numbers of APs being paired with EPSPs in a burst and examined the amount of LTP in each group (Fig. 7*B*). LTP could be induced in *Kv4.2*$^{-/-}$ when less than one AP on average was paired with the EPSPs (1.72 ± 0.29; $n = 4$). In wild-type littermate controls when the number of paired APs was minimal (0.5–0.9 per burst on average), EPSP initial slope remained mostly unchanged after induction (1.00 ± 0.13; $n = 5$). Thus in wild-type animals LTP could be induced only when >1.5 APs on average were paired with EPSPs. Specifically, 1 to 1.9 AP and 2 to 2.9 AP induction protocols resulted in 1.36 ± 0.16-fold ($n = 14$) and 1.94 ± 0.33-fold ($n = 5$) changes in EPSP initial slope in wild-type neurons, respectively. LTP magnitude increased as the number of paired APs increased and reached its maximal level at three to five APs (2.53 ± 0.28; $n = 9$). However, the amount of LTP appeared already to exhibit a maximum plateau level with two APs in *Kv4.2*$^{-/-}$ (2.78 ± 0.6-fold change in EPSP slope; $n = 5$). If we operationally define the "induction threshold of LTP" as the required minimum numbers of APs that are paired with EPSPs, then in *Kv4.2*$^{-/-}$ the induction threshold of LTP was significantly lower than in wild-type animals.

Discussion

Many types of cells in a variety of species express a voltage-dependent K^+ current with rapid activation and inactivation (Coetzee et al., 1999). These transient K^+ currents collectively are called the "A-type K^+ currents." Their importance in electrical

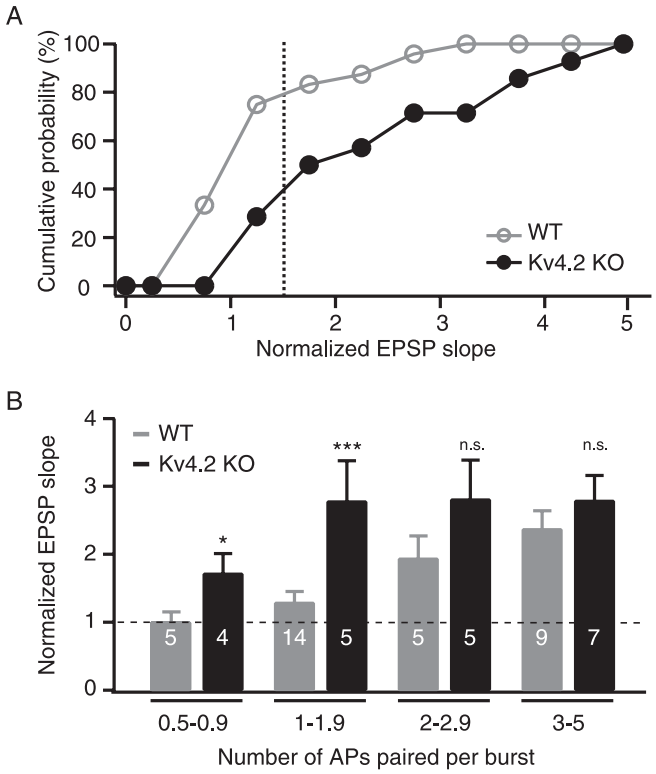

Figure 7. The induction threshold of LTP was lower in *Kv4.2* $^{-/-}$ than in control littermates. ***A***, Cumulative probability plot showing higher probability of LTP induction in *Kv4.2* $^{-/-}$ than in control littermates, when a weak (<2 AP–EPSP pairings) TBP protocol was used. The dotted line indicates a 50% increase of EPSP slope. ***B***, Amount of LTP was plotted against the number of AP–EPSP pairings and compared between *Kv4.2* $^{-/-}$ and wild-type (WT) littermate controls. Pairing fewer than two APs (0.5–0.9 and 1–1.9 groups) with EPSPs was sufficient to induce LTP in *Kv4.2* $^{-/-}$, but not in control, animals. Stronger protocols consisting of two to 2.9 APs or three to five APs resulted in robust LTP in both genotypes, and the amount of LTP was not statistically different. Error bars represent the SEM; *$p < 0.05$; ***$p < 0.005$; n.s., not significant, $p > 0.05$. The number of cells in each group is indicated in the bars of the graph.

signaling has motivated significant research effort in elucidating their molecular identities in different types of cells (Guo et al., 2005; Hu et al., 2006).

Several lines of evidence point to the A-type K^+ current as a key regulator of action potential backpropagation in the CA1 pyramidal neurons. First, the progressive decrease of bAP amplitude parallels the increase of A-type K^+ current density along the length of the apical dendrites (Hoffman et al., 1997). Second, the amplitude of dendritic bAP is increased greatly by 5–10 mM 4-aminopyridine (Hoffman et al., 1997). Although a nonspecific drug, 4-aminopyridine preferentially blocks the A-type K^+ current in CA1 neurons (Storm, 1990; Hoffman et al., 1997). Third, activation of cAMP-dependent protein kinase (PKA) or protein kinase C (PKC) downregulates A-type K^+ current by shifting the activation curve to a more depolarized voltage range (Hoffman and Johnston, 1998). Activation of PKA or PKC also increases the amplitude of dendritic bAPs (Hoffman and Johnston, 1998; Yuan et al., 2002). Similarly, inhibition of the MAP (mitogen-activated protein) kinase pathway upregulates A-type K^+ current by shifting the activation curve to a more hyperpolarized voltage range (Watanabe et al., 2002). The same manipulation results in a decrease of bAP amplitude (Watanabe et al., 2002; Yuan et al., 2002) and suppression of LTP induction (Watanabe et al., 2002). The dendritic A-type K^+ current also underlies changes in local dendritic excitability during the expression of LTP (Frick et al., 2004). In addition, the dendritic A-type K^+ current appears to be downregulated in an animal model of temporal lobe epilepsy, a condition in which bAPs are found to have less decrement in their dendrites (Bernard et al., 2004).

The *Kv4.2* gene encodes a transient A-type channel in heterologous expression systems (Baldwin et al., 1991), and, immunohistochemically, Kv4.2 proteins are located preferentially in the dendrites of hippocampal neurons (Sheng et al., 1992). Hence we hypothesized that the *Kv4.2* gene encodes the pore-forming α-subunit of dendritic A-type K^+ current in CA1. This hypothesis predicts an absence of A-type K^+ current in CA1 dendrites of *Kv4.2* $^{-/-}$ animals.

With dendritic cell-attached voltage-clamp recordings we found that the A-type component of dendritic K^+ currents in *Kv4.2* $^{-/-}$ mice was essentially absent, whereas other components of voltage-dependent K^+ currents in the dendrites were intact. The elimination of A-type K^+ current was complete in the dendrite, but not in the whole cell. Upregulation of Kv1-mediated channels may compensate for the loss of Kv4.2 in parts of the cell other than the apical dendrite (Fig. 2). A small but significant upregulation of Kv1.4 protein was demonstrated in ventricular cardiac myocytes of *Kv4.2* $^{-/-}$ mice (Guo et al., 2005). We did not detect a significant upregulation of Kv1.4 protein in the hippocampus with Western blotting. However, this upregulation may be occurring in CA1 pyramidal neurons but may be harder to detect with Western blotting against a background of Kv1.4 expression in other hippocampal cell types. In addition, although an upregulation of Kv1 proteins may compensate for the loss of whole-cell A-type current, the ability of the neuron to compensate may be limited by the fact that it apparently cannot send Kv1 proteins to the dendrites (Gu et al., 2003). Although our data support dendritic A-type current being composed of Kv4.2, we cannot exclude the alternative possibility that downregulation of proteins other than Kv4.2 (KChIPs, for example) (Fig. 1) may have caused concomitant downregulation of channel proteins other than Kv4.2. However, our Western blotting data demonstrate no downregulation of Kv4.3, the principal alternative candidate molecule that might encode dendritic A-type current. It also would be of great interest to explore whether meaningful functional links exist between the downregulation of Kv4.2 and KChIPs (Menegola and Trimmer, 2006). Nevertheless, we believe the most straightforward interpretation of our data is that Kv4.2 is a necessary α-subunit for the dendritic A-type K^+ current in CA1.

The specific and complete elimination of A-type K^+ current in the CA1 dendrites of *Kv4.2* $^{-/-}$ mice provided the basis for our interpretation of subsequent experiments. We demonstrated that APs in CA1 pyramidal neurons backpropagate into the dendrites with a decrement in amplitude. This decrement was reduced in *Kv4.2* $^{-/-}$ dendrites, but was not completely absent. In other words, complete elimination of A-type K^+ current in dendrites did not fully restore bAPs to the same amplitude of somatic APs. This observation suggests that other mechanisms also are involved in regulation of bAP, such as dendritic morphology and geometry (Williams and Stuart, 2000; London and Hausser, 2005).

The bigger-amplitude bAPs were accompanied by Ca^{2+} influx, which decreased much less in the dendrites of *Kv4.2* $^{-/-}$ animals than in the dendrites of wild-type animals. As a consequence, induction of Hebbian-type LTP was easier in *Kv4.2* $^{-/-}$ neurons because fewer postsynaptic APs were required to induce robust LTP. Previous studies with selective blockers of Kv4 channels using field recordings reported qualitatively similar results

(Ramakers and Storm, 2002). In our studies the maximum amount of LTP was not significantly different between *Kv4.2*$^{-/-}$ and wild-type animals. It is interesting to consider that the induction of long-term depression (LTD), another form of neural plasticity, also depends on the amount of Ca^{2+} influx. It remains to be tested whether larger bAPs propagating in the dendrites of *Kv4.2*$^{-/-}$ also exert their influence on LTD induction.

Given the results of previous studies (Hoffman et al., 1997; Bernard et al., 2004), it came as a surprise that the *Kv4.2*$^{-/-}$ animals did not have innate epilepsy with a behavioral manifestation. We think perhaps the upregulation of the Kv1-mediated current could have played a compensatory role to counter the expected increase in whole-cell excitability in *Kv4.2*$^{-/-}$. However, it remains to be seen whether epileptic forms of activity can be recorded with EEGs in the *Kv4.2*$^{-/-}$ animals and whether the *Kv4.2*$^{-/-}$ animals are more prone to epilepsy when challenged with exogenous insults.

In conclusion, the *Kv4.2*$^{-/-}$ mice have proven to be a useful model for establishing a causal link between a dendritic conductance (A-type K^+ current), aspects of neuronal signaling and plasticity (London and Hausser, 2005), and a specific molecule, Kv4.2. Together with previous research (Hoffman et al., 1997; Hoffman and Johnston, 1998; Ramakers and Storm, 2002; Watanabe et al., 2002; Yuan et al., 2002; Frick et al., 2004), our data provide strong support for A-type K^+ current determining action potential backpropagation in the dendrites and regulating the induction threshold of synaptic plasticity. However, the A-type K^+ current is not the complete story, as we show in the case of action potential backpropagation, and additional experiments are necessary to delineate fully the mechanisms regulating signal propagation in dendrites.

References

Baldwin TJ, Tsaur ML, Lopez GA, Jan YN, Jan LY (1991) Characterization of a mammalian cDNA for an inactivating voltage-sensitive K^+ channel. Neuron 7:471–483.

Bernard C, Johnston D (2003) Distance-dependent modifiable threshold for action potential back-propagation in hippocampal dendrites. J Neurophysiol 90:1807–1816.

Bernard C, Anderson A, Becker A, Poolos NP, Beck H, Johnston D (2004) Acquired dendritic channelopathy in temporal lobe epilepsy. Science 305:532–535.

Bi GQ, Poo MM (1998) Synaptic modifications in cultured hippocampal neurons: dependence on spike timing, synaptic strength, and postsynaptic cell type. J Neurosci 18:10464–10472.

Castellino RC, Morales MJ, Strauss HC, Rasmusson RL (1995) Time- and voltage-dependent modulation of a Kv1.4 channel by a β-subunit (Kvβ3) cloned from ferret ventricle. Am J Physiol 269:H385–H391.

Chen X, Johnston D (2004) Properties of single voltage-dependent K^+ channels in dendrites of CA1 pyramidal neurones of rat hippocampus. J Physiol (Lond) 559:187–203.

Chen X, Johnston D (2006) Voltage-gated ion channels in dendrites of hippocampal pyramidal neurons. Pflügers Arch, in press.

Coetzee WA, Amarillo Y, Chiu J, Chow A, Lau D, McCormack T, Moreno H, Nadal MS, Ozaita A, Pountney D, Saganich M, Vega-Saenz de Miera E, Rudy B (1999) Molecular diversity of K^+ channels. Ann NY Acad Sci 868:233–285.

Colbert CM, Johnston D (1996) Axonal action potential initiation and Na^+ channel densities in the soma and axon initial segment of subicular pyramidal neurons. J Neurosci 16:6676–6686.

Debanne D, Gahwiler BH, Thompson SM (1998) Long-term synaptic plasticity between pairs of individual CA3 pyramidal cells in rat hippocampal slice cultures. J Physiol (Lond) 507:237–247.

Fan Y, Fricker D, Brager DH, Chen X, Lu HC, Chitwood RA, Johnston D (2005) Activity-dependent decrease of excitability in rat hippocampal neurons through increases in I_h. Nat Neurosci 8:1542–1551.

Frick A, Magee J, Koester HJ, Migliore M, Johnston D (2003) Normalization of Ca^{2+} signals by small oblique dendrites of CA1 pyramidal neurons. J Neurosci 23:3243–3250.

Frick A, Magee J, Johnston D (2004) LTP is accompanied by an enhanced local excitability of pyramidal neuron dendrites. Nat Neurosci 7:126–135.

Golding NL, Staff NP, Spruston N (2002) Dendritic spikes as a mechanism for cooperative long-term potentiation. Nature 418:326–331.

Gu C, Jan YN, Jan LY (2003) A conserved domain in axonal targeting of Kv1 (Shaker) voltage-gated potassium channels. Science 301:646–649.

Guo W, Jung WE, Marionneau C, Aimond F, Xu H, Yamada KA, Schwarz TL, Demolombe S, Nerbonne JM (2005) Targeted deletion of Kv4.2 eliminates $I_{to,f}$ and results in electrical and molecular remodeling, with no evidence of ventricular hypertrophy or myocardial dysfunction. Circ Res 97:1342–1350.

Hoffman DA, Johnston D (1998) Downregulation of transient K^+ channels in dendrites of hippocampal CA1 pyramidal neurons by activation of PKA and PKC. J Neurosci 18:3521–3528.

Hoffman DA, Magee JC, Colbert CM, Johnston D (1997) K^+ channel regulation of signal propagation in dendrites of hippocampal pyramidal neurons. Nature 387:869–875.

Hu HJ, Carrasquillo Y, Karim F, Jung WE, Nerbonne JM, Schwarz TL, Gereau 4th RW (2006) The Kv4.2 potassium channel subunit is required for pain plasticity. Neuron 50:89–100.

Jaffe DB, Ross WN, Lisman JE, Lasser-Ross N, Miyakawa H, Johnston D (1994) A model for dendritic Ca^{2+} accumulation in hippocampal pyramidal neurons based on fluorescence imaging measurements. J Neurophysiol 71:1065–1077.

Jerng HH, Qian Y, Pfaffinger PJ (2004) Modulation of Kv4.2 channel expression and gating by dipeptidyl peptidase 10 (DPP10). Biophys J 87:2380–2396.

Jeromin A, Yuan LL, Frick A, Pfaffinger P, Johnston D (2003) A modified Sindbis vector for prolonged gene expression in neurons. J Neurophysiol 90:2741–2745.

Johnston D, Brown TH (1983) Interpretation of voltage-clamp measurements in hippocampal neurons. J Neurophysiol 50:464–486.

Johnston D, Hoffman DA, Magee JC, Poolos NP, Watanabe S, Colbert CM, Migliore M (2000) Dendritic potassium channels in hippocampal pyramidal neurons. J Physiol (Lond) 525:75–81.

Jung WE (2002) Characterization of mice lacking Kv4.2, an A-type potassium channel. PhD thesis, Stanford University.

Koester HJ, Sakmann B (1998) Calcium dynamics in single spines during coincident pre- and postsynaptic activity depend on relative timing of back-propagating action potentials and subthreshold excitatory postsynaptic potentials. Proc Natl Acad Sci USA 95:9596–9601.

Lisman J, Spruston N (2005) Postsynaptic depolarization requirements for LTP and LTD: a critique of spike timing-dependent plasticity. Nat Neurosci 8:839–841.

London M, Hausser M (2005) Dendritic computation. Annu Rev Neurosci 28:503–532.

Magee JC, Johnston D (1995) Characterization of single voltage-gated Na^+ and Ca^{2+} channels in apical dendrites of rat CA1 pyramidal neurons. J Physiol (Lond) 487:67–90.

Magee JC, Johnston D (1997) A synaptically controlled, associative signal for Hebbian plasticity in hippocampal neurons. Science 275:209–213.

Mainen ZF, Malinow R, Svoboda K (1999) Synaptic calcium transients in single spines indicate that NMDA receptors are not saturated. Nature 399:151–155.

Markram H, Lübke J, Frotscher M, Sakmann B (1997) Regulation of synaptic efficacy by coincidence of postsynaptic APs and EPSPs. Science 275:213–215.

Menegola M, Trimmer JS (2006) Unanticipated region- and cell-specific downregulation of individual KChIP auxiliary subunit isotypes in Kv4.2 knock-out mouse brain. J Neurosci 26:12137–12142.

Nevian T, Sakmann B (2004) Single spine Ca^{2+} signals evoked by coincident EPSPs and backpropagating action potentials in spiny stellate cells of layer 4 in the juvenile rat somatosensory barrel cortex. J Neurosci 24:1689–1699.

Ramakers GM, Storm JF (2002) A postsynaptic transient K^+ current modulated by arachidonic acid regulates synaptic integration and threshold for LTP induction in hippocampal pyramidal cells. Proc Natl Acad Sci USA 99:10144–10149.

Regehr WG, Tank DW (1992) Calcium concentration dynamics produced by synaptic activation of CA1 hippocampal pyramidal cells. J Neurosci 12:4202–4223.

Rhodes KJ, Carroll KI, Sung MA, Doliveira LC, Monaghan MM, Burke SL, Strassle BW, Buchwalder L, Menegola M, Cao J, An WF, Trimmer JS (2004) KChIPs and Kv4α subunits as integral components of A-type potassium channels in mammalian brain. J Neurosci 24:7903–7915.

Schiller J, Helmchen F, Sakmann B (1995) Spatial profile of dendritic calcium transients evoked by action potentials in rat neocortical pyramidal neurones. J Physiol (Lond) 487:583–600.

Sheng M, Tsaur ML, Jan YN, Jan LY (1992) Subcellular segregation of two A-type K^+ channel proteins in rat central neurons. Neuron 9:271–284.

Sjostrom PJ, Turrigiano GG, Nelson SB (2001) Rate, timing, and cooperativity jointly determine cortical synaptic plasticity. Neuron 32:1149–1164.

Spruston N, Schiller Y, Stuart G, Sakmann B (1995) Activity-dependent action potential invasion and calcium influx into hippocampal CA1 dendrites. Science 268:297–300.

Stoppini L, Buchs PA, Muller D (1991) A simple method for organotypic cultures of nervous tissue. J Neurosci Methods 37:173–182.

Storm JF (1990) Potassium currents in hippocampal pyramidal cells. Prog Brain Res 83:161–187.

Stuart GJ, Hausser M (2001) Dendritic coincidence detection of EPSPs and action potentials. Nat Neurosci 4:63–71.

Stuart GJ, Sakmann B (1994) Active propagation of somatic action potentials into neocortical pyramidal cell dendrites. Nature 367:69–72.

Varga AW, Yuan LL, Anderson AE, Schrader LA, Wu GY, Gatchel JR, Johnston D, Sweatt JD (2004) Calcium-calmodulin-dependent kinase II modulates Kv4.2 channel expression and upregulates neuronal A-type potassium currents. J Neurosci 24:3643–3654.

Watanabe S, Hoffman DA, Migliore M, Johnston D (2002) Dendritic K^+ channels contribute to spike-timing-dependent long-term potentiation in hippocampal pyramidal neurons. Proc Natl Acad Sci USA 99:8366–8371.

Williams SR, Stuart GJ (2000) Action potential backpropagation and somato-dendritic distribution of ion channels in thalamocortical neurons. J Neurosci 20:1307–1317.

Yuan LL, Adams JP, Swank M, Sweatt JD, Johnston D (2002) Protein kinase modulation of dendritic K^+ channels in hippocampus involves a mitogen-activated protein kinase pathway. J Neurosci 22:4860–4868.

Yuste R, Denk W (1995) Dendritic spines as basic functional units of neuronal integration. Nature 375:682–684.